UNLIMITED

TR 88058

ROYAL AEROSPACE ESTABLISHMENT

Technical Report 88058

September 1988

ORBIT DETERMINATION AND ANALYSIS FOR COSMOS 236 AT 15th-ORDER RESONANCE

by

A. N. Winterbottom

Procurement Executive, Ministry of Defence
Farnborough, Hants

UNLIMITED

UNLIMITED

ROYAL AEROSPACE ESTABLISHMENT

Technical Report 88058

Received for printing 6 September 1988

ORBIT DETERMINATION AND ANALYSIS FOR COSMOS 236 AT 15TH-ORDER RESONANCE

by

A. N. Winterbottom

SUMMARY

Cosmos 236 (1968-70A) was launched on 27 August 1968 into a near-circular orbit of inclination 56° and is expected to decay during late 1989. The orbit has been determined from observations for 77 epochs between July 1983 and October 1984 over the time interval when the orbit was expected to be significantly influenced by the effects of 15th-order resonance with the Earth's gravitational field: exact resonance occurred on 13 March 1984. The observations numbered over 4700, including 284 from the Hewitt cameras of the University of Aston which are sited at Herstmonceux in England and at Siding Spring in Australia. The orbital accuracy achieved was fairly consistent throughout, with the standard deviation in orbital inclination and eccentricity corresponding on average to positional accuracies of 85 m and 65 m respectively.

Analysis of the changes in inclination and in eccentricity at resonance has given values of three pairs of lumped harmonics of order 15 and three pairs of order 30, one pair of each from inclination and two from eccentricity. The values from inclination had standard deviations equivalent to accuracies in geoid height of 0.6 cm and 2.0 cm for orders 15 and 30 respectively while the equivalent accuracies for the values from eccentricity were 1.6 cm and 6.0 cm.

Departmental Reference: SS 9

UNLIMITED

LIST OF CONTENTS

1 INTRODUCTION

The satellite Cosmos 236, designated 1968-70A, was launched on 27 August 1968 and is expected to decay in the Earth's atmosphere during the last half of 1989. It is cylindrical in shape, about 2 m long and 1 m diameter, with a weight of about 850 kg and its initial orbital parameters[1] were: inclination 56.07°, perigee and apogee heights 588 and 630 km respectively, and nodal period 96.83 minutes.

The orbit of Cosmos 236 contracted slowly under the influence of air drag, and in March 1984 it passed through 15th-order resonance, which occurs when a satellite's track over the Earth repeats after 15 revolutions, *ie* when the satellite makes 15 revolutions while the Earth spins once relative to the orbital plane. If the passage through resonance is slow enough, the effects of 15th-order harmonics in the geopotential can build up and result in an appreciable perturbation to some of the orbital elements: this variation can be analysed to derive values for lumped geopotential harmonics of order 15. The orbit of Cosmos 236 has been determined between July 1983 and October 1984 from radar and optical observations with the aid of the RAE orbit refinement program[2] PROP6, and the changes in inclination and eccentricity have been analysed to give six values of lumped 15th-order harmonics and six of 30th-order.

2 THE OBSERVATIONS AND THE ORBITS

2.1 Sources of the observations

The orbit of 1968-70A has been determined at 77 epochs between 4 July 1983 and 30 October 1984 from 4744 observations, not including those rejected in the orbit determinations.

The observations came from three different sources, the most accurate being those from the University of Aston's Hewitt cameras at the Royal Greenwich Observatory, Herstmonceux, and at Siding Spring in Australia; 284 of these observations were used in 33 of the 77 orbits. The second group consisted of 282 visual observations made by volunteer observers reporting to the Earth Satellite Research Unit at the University of Aston. The third and largest group were 4178 radar observations made by the US Navy Navspasur system, kindly supplied by the US Naval Research Laboratory.

2.2 Observational accuracy

The rms residuals of the observations have been calculated using the RAE computer program ORES[3] and have been sent to the observers. Table 1 gives the

058

residuals for selected observing stations with at least six observations accepted in the final orbit determinations. The US Navy observations are geocentric, and if they were given in the same form as the topocentric observations, their angular rms residuals would increase by a factor of between 5 and 10. In calculating the rms residuals for the visual observers, observations with residuals greater than twice the rms have been omitted, the numbers used being shown in brackets. This gives a truer impression of the normal accuracy of the observer, as it eliminates observations marred by poor seeing conditions and possible deficiencies in orbital fitting.

Table 1

Residuals for selected stations

Station		Number of accepted observations	rms residuals			
			Range km	Minutes of arc		
				RA	Dec	Total
1	US Navy	565		2.2	1.7	2.8
2	US Navy	338		2.9	3.0	4.2
3	US Navy	395		3.1	2.4	3.9
4	US Navy	533		3.1	2.7	4.2
5	US Navy	369		2.6	2.2	3.4
6	US Navy	554		2.3	1.9	3.0
29	US Navy	1424	0.6	0.3*	0.2*	
414	Capetown	12(11)		1.7	1.7	2.4
2122	Malvern 5	11		2.0	1.6	2.6
2265	Farnham	6(5)		3.2	2.5	4.0
2414	Bournemouth	112(104)		4.0	4.2	5.8
2418	Sunningdale	15		4.1	4.5	6.1
2420	Willowbrae	54(51)		7.9	3.9	8.8
2437	Warrington	12		5.8	6.3	8.6
2539	Dymchurch	15(14)		2.0	1.6	2.6
2657	Bridgwater	10		1.6	2.4	2.9
2659	Herstmonceux 3 (Hewitt camera)	266(250)		0.11	0.06	0.13
4156	Apeldoorn	14(12)		3.1	2.6	4.1
9652	Siding Spring (Hewitt camera)	18		0.04	0.04	0.05

* Geocentric

The rms residuals of the Hewitt cameras are 8 seconds of arc from 250 observations by the Herstmonceux camera and 3 seconds of arc from 18 observations by the Siding Spring camera, equivalent to about 30 and 10 m in position respectively. The accuracy in plate reading is usually estimated as about 2 seconds of arc and the residuals for Siding Spring confirm this estimate. The residual is of course a combination of (a) observational error and (b) errors in the orbital model and the orbit determination process. A number of the orbits utilized more

than one plate from the Herstmonceux camera, and the PROP orbital model, which ignores lunisolar perturbations, is not accurate enough to do justice to the multiple plates in one orbit determination: lunisolar perturbations can build up to the order of 50-100 m in a week, much greater than the 5-10 m capability of the cameras. The Herstmonceux camera residuals are therefore as good as could be expected with PROP.

2.3 The orbits

The orbits have been determined with the aid of the RAE orbit refinement program PROP in the PROP6 version, and the orbital elements at the 77 epochs, with their standard deviations, are given in Table 2 (page 17). The epoch for each orbit is at 00 hours on the day indicated, and the PROP program fits the mean anomaly M by a polynomial of the form

$$M = M_0 + M_1 t + M_2 t^2 + M_3 t^3 + M_4 t^4 + M_5 t^5 \qquad (1)$$

where t is the time measured from epoch. Up to six M-coefficients may be used, depending on the severity of the drag. For 1968-70A, which at resonance was in a near-circular orbit at a height of about 500 km, $M_0 - M_2$ were sufficient for 59 of the orbits, and 18 orbits required $M_0 - M_3$.

All of the orbits fitted the observations satisfactorily, with the value of ε, the parameter which indicates the measure of fit, varying from 0.26 to 0.90 with an average value of 0.53. The average number of observations in an orbit determination was 62, spread over a time interval averaging 5.9 days.

The average standard deviation in eccentricity for all the 77 orbits is 0.000009, equivalent to an error in perigee distance of 65 m, and this is much the same as the average standard deviation for the 33 orbits containing Hewitt camera observations. As the eccentricity is very small, it is useful to plot the values in polar form, as shown in Fig 1, where the values are linked with a continuous line as a guide to the eye. In the absence of drag and resonance, the locus of the points should be close to a circle; when drag acts, the circle is converted to a contracting spiral[4]. In Fig 1, however, the initial circuit (orbits 1-29) is followed by a second (orbits 30-57) which spirals outwards, presumably as a result of the resonance. (Thus it might be guessed, even from the raw values of Fig 1, that the resonance begins to act strongly at about orbit 29.) The third circuit closely follows the first between orbits 61 and 71.

058

The mean standard deviation in inclination for the 77 orbits is 0.0007°, corresponding to an error of about 85 m in cross-track distance; for the 33 orbits with Hewitt camera observations the accuracy is better, the average standard deviation being 0.0005°.

3 RESONANCE THEORY

The theory has often been given (*eg* Ref 5) and will only be outlined here. In brief, the rate of change of inclination i caused by a relevant pair of geopotential coefficients $\bar{C}_{\ell m}$ and $\bar{S}_{\ell m}$ near resonance may be written

$$\frac{di}{dt} = \frac{n\left(1 - e^2\right)^{-\frac{1}{2}}}{\sin i}\left(\frac{R}{a}\right)^{\ell} \bar{F}_{\ell mp} G_{\ell pq}(k \cos i - m)\mathcal{R}\left[j^{\ell-m+1}\left(\bar{C}_{\ell m} - j\bar{S}_{\ell m}\right) \exp\left\{j(\gamma\Phi - q\omega)\right\}\right] \qquad \ldots\ldots (2)$$

where F and G are functions of inclination and eccentricity defined in Ref 5, R is the Earth's equatorial radius, and the resonance angle Φ for 15:1 resonance is given by

$$\Phi = \omega + M + 15(\Omega - \nu) \qquad (3)$$

where ν is the sidereal angle. The indices γ and q are integers, and in practice the most important terms are those with $\gamma = 1$, though those with $\gamma = 2$ may also be needed. For inclination, the $q = 0$ terms are the most important, but the eccentricity is affected most by the terms with $q = \pm 1$. For 15:1 resonance the equations linking m, γ, q, k, p and ℓ are: $m = 15\gamma$; $k = \gamma - q$; $2p = \ell - k$. The values of ℓ must be such that $\ell \geqslant m$ and $(\ell - k)$ is even. The successive $\bar{C}_{\ell m}$ and $\bar{S}_{\ell m}$ coefficients that arise may be grouped into a 'lumped harmonic',

$$\bar{C}_m^{q,k} = \sum_{\ell} Q_{\ell}^{q,k}\bar{C}_{\ell m}, \quad \bar{S}_m^{q,k} = \sum_{\ell} Q_{\ell}^{q,k}\bar{S}_{\ell m}, \qquad (4)$$

where ℓ increases in steps of 2 from its minimum value ℓ_0 and the Q_ℓ are constant coefficients. Thus the observed change in i at resonance gives values of the lumped harmonics $\bar{C}_m^{q,k}$ and $\bar{S}_m^{q,k}$ appropriate to a particular inclination, here 56.08°. When values are available for many different inclinations, the individual harmonics can be determined[6].

The rate of change of eccentricity produced by the (ℓ,m) harmonics is given by[5]:

$$\frac{de}{dt} = n\left(\frac{R}{a}\right)^{\ell} \bar{F}_{\ell mp} G_{\ell pq} \left\{\frac{q - \frac{1}{2}(k + 3q)e^2}{e}\right\} \mathscr{R}\left[j^{\ell-m+1}\left(\bar{C}_{\ell m} - j\bar{S}_{\ell m}\right) \exp j(\gamma\Phi - q\omega)\right] \quad .....(5)$$

Again the $\bar{C}_{\ell m}$ and $\bar{S}_{\ell m}$ may be grouped into appropriate lumped harmonics.

4 THE PASSAGE THROUGH RESONANCE FOR COSMOS 236

Exact resonance, $\dot{\Phi} = 0$, occurred on 13 March 1984, and the variation of $\dot{\Phi}$ and Φ with time is shown in Fig 2. It can be seen that $\dot{\Phi}$ increases fairly steadily between -6.8 degrees/day initially and +5.3 degrees/day at the end, so the resonance is well balanced and does not suffer from the considerable changes in drag which affect many resonance analyses. This good balance is due to the fortunate chance that resonance occurred at a time close to the minimum of the solar cycle, when air density was at its lowest and fairly steady.

5 ANALYSIS OF INCLINATION

Two important perturbations need to be subtracted from the raw values of inclination in Table 2. The first is that due to the combined effect of lunisolar and zonal harmonic perturbations, which were calculated using the RAE computer program PROD[7], with a 1-day integration interval and restarts every 20 days or less. The second is that due to the $J_{2,2}$ tesseral harmonic, which is printed on each orbit determination output by the PROP program. These two perturbations, which had maximum numerical values of 0.0024° and 0.0017° respectively, were subtracted from the raw values. Perturbations due to tides and solar radiation pressure were considered too small to be worth evaluating. The resulting values of inclination, with standard deviations, are shown in Fig 3: the main change due to resonance and the subsidiary oscillations are well displayed.

The values were then fitted with an integrated form of the theoretical equation (2) with the aid of the THROE computer program[8], for various pairs of (γ,q) , assuming an atmospheric rotation rate[9] of 0.9 rev/day; a minimum standard deviation of 0.0005° was set, in view of the neglect of earth and ocean tides. The THROE program adjusts the values of i for the effects of atmospheric rotation and lunisolar precession of the Earth's axis.

As a result of previous analyses of inclination[10] for near-circular orbits at 15th-order resonance, it was expected that the most important pairs of values of (γ,q) would be $(\gamma,q) = (1,0)$ and $(2,0)$ with the possible additional pairs $(\gamma,q) = (1,1)$ and $(1,-1)$. Here it was found that there was no advantage in

using the additional pairs because the fitting was not substantially improved and the lumped values derived were indeterminate. For similar reasons the addition of $(\gamma,q) = (3,0)$ terms was unavailing. The fitting was therefore made with $(\gamma,q) = (1,0)$ and $(2,0)$ only: the nominal standard deviations were doubled on eight orbits* to avoid residuals of more than twice the measure of fit ε , and one standard deviation (for MJD 45872) had to be quadrupled, for the same reason.

The THROE fitting of the theoretical curve to the observed values is shown in Fig 4; the orbits mentioned above are shown with their relaxed standard deviations. The measure of fit ε had the value 1.49 and the values of the lumped harmonics obtained were as follows:

$$10^9\bar{C}_{15}^{0,1} = -213.5 \pm 5.4 \qquad 10^9\bar{S}_{15}^{0,1} = -91.1 \pm 4.2$$

$$10^9\bar{C}_{30}^{0,2} = -34 \pm 149 \qquad 10^9\bar{S}_{30}^{0,2} = -624 \pm 106 \quad . \tag{6}$$

The fitting in Fig 4 is very good, and the values derived should be reliable. The value of ε substantially greater than 1 implies either that the standard deviations are slightly overoptimistic, or that the modelling has some small imperfections.

6 ANALYSIS OF ECCENTRICITY

The lunisolar perturbations to eccentricity e have been obtained using the PROD program, and have been removed. The air drag effects have been removed within THROE, assuming a constant scale height H of 60 km, appropriate to a height of 490 km, and taking mean values of M_2 between successive orbits[11]. The zonal harmonic perturbations were also removed within THROE and it was found that a small adjustment to the odd zonal harmonic oscillation, expressed as a change in $10^6 J_3$ from -2.53 to -2.60, was beneficial in improving the fitting.

The values of e thus obtained are shown in Fig 5, which also gives the final THROE fitting, with $(\gamma,q) = (1,1)$, $(1,-1)$, $(2,1)$ and $(2,-1)$. It is immediately apparent in Fig 5 that the THROE fitting is deficient between MJD 45782 and 45818, orbits 44-50, and Fig 1 shows that this is just the region where e becomes extremely small and $\dot{\omega}$ varies greatly (ω decreases by 115° in 5 days between orbits 50 and 51). THROE is not fully adapted for avoiding problems when e is very small, because it is formulated in terms of e and ω ,

* At MJD 45519, 45523, 45531, 45647, 45654, 45751, 45805, 45978.

058

rather than $e \cos \omega$ and $e \sin \omega$, as is necessary for very small e. Thus the reliability of the results from this fitting is open to question, although it may be that the high value of the measure of fit will in itself provide sufficient allowance for the ill-fitting region. In the fitting the seven values between MJD 45782 and 45818 were all relaxed, the first, sixth and seventh by a factor of 2 and the others by a factor of 4, to avoid residuals $>2\varepsilon$. Apart from this 'problem region', it was only necessary to relax three values by a factor of 2 (MJD 45536, 45597 and 45654) and one by a factor of 4 (MJD 45527). With these standard deviations, which are indicated in Fig 5, the measure of fit ε was 2.63 and the values of the lumped harmonics obtained were:

$$10^9\bar{C}_{15}^{1,0} = 20.4 \pm 10.2 \qquad 10^9\bar{S}_{15}^{1,0} = 39.3 \pm 7.6$$

$$10^9\bar{C}_{15}^{-1,2} = 74.4 \pm 5.8 \qquad 10^9\bar{S}_{15}^{-1,2} = 37.5 \pm 4.4$$

$$10^9\bar{C}_{30}^{1,1} = -343 \pm 121 \qquad 10^9\bar{S}_{30}^{1,1} = -116 \pm 234$$

$$10^9\bar{C}_{30}^{-1,3} = 553 \pm 77 \qquad 10^9\bar{S}_{30}^{-1,3} = 509 \pm 117 \quad . \tag{7}$$

In several recent analyses of eccentricity at 15th-order resonance the effect of the day-to-night variation in density has been taken into account. Here this effect is quite small, as indicated in section 8, and has not been taken into account.

7 INCLINATION AND ECCENTRICITY FITTED SIMULTANEOUSLY

The changes in inclination and eccentricity have been fitted simultaneously with the aid of R.H. Gooding's program SIMRES. It was not expected that better values would emerge, because the sets of lumped harmonics obtained from i are completely different from those obtained from e ; but the simultaneous fitting seemed worth trying.

As usual, the inclination and eccentricity were weighted in accordance with the ε values of the contributing THROE runs, and the values obtained for the six pairs of lumped harmonics are:

058

$$10^9\bar{C}_{15}^{0,1} = -211.1 \pm 5.2 \qquad 10^9\bar{S}_{15}^{0,1} = -87.3 \pm 4.0$$

$$10^9\bar{C}_{30}^{0,2} = 65 \pm 143 \qquad 10^9\bar{S}_{30}^{0,2} = -624 \pm 104$$

$$10^9\bar{C}_{15}^{1,0} = 19.3 \pm 10.4 \qquad 10^9\bar{S}_{15}^{1,0} = 39.3 \pm 7.7$$

$$10^9\bar{C}_{15}^{-1,2} = 74.8 \pm 6.0 \qquad 10^9\bar{S}_{15}^{-1,2} = 37.0 \pm 4.5$$

$$10^9\bar{C}_{30}^{1,1} = -347 \pm 123 \qquad 10^9\bar{S}_{30}^{1,1} = -114 \pm 238$$

$$10^9\bar{C}_{30}^{-1,3} = 559 \pm 78 \qquad 10^9\bar{S}_{30}^{-1,3} = 507 \pm 118 \quad . \qquad (8)$$

It will be seen that the last four pairs of values are virtually the same as in equations (7) derived from eccentricity alone, though the standard deviations are marginally greater: this is to be expected, because the first two pairs of values have very little influence on the eccentricity. The first two pairs of values are, however, appreciably different from those obtained from inclination alone, equations (6), the largest change (for $\bar{S}_{15}^{0,1}$) being 0.9 sd. Again this is to be expected, because the other four pairs, the values of which are in effect 'imposed' by e, do have a slight influence on i. If the values obtained from e were fully reliable, the SIMRES solution would be preferred; as the e-analysis is slightly questionable, however, the separate solutions, equations (6) and (7), have to be recommended. (It is therefore a little ironical that in the solutions for individual coefficients[6], the SIMRES values of $\bar{S}_{15}^{0,1}$ and $\bar{C}_{30}^{0,2}$ fit better, though $\bar{C}_{15}^{0,1}$ fits worse.)

8 THE EFFECT OF THE DAY-TO-NIGHT VARIATION IN AIR DENSITY

The day-to-night variation in air density has an effect on eccentricity, but has been neglected and needs to be approximately estimated. When $e < 0.003$, as it is here, the decrease in e per revolution due to drag is given by equation (11.11) of Ref 4 as

$$\Delta e = -\pi\delta a\rho_o \exp\left\{\left(r_o - a\right)/H\right\}\left[z + F\cos\phi_p + O\left(e, \tfrac{1}{4}z^2\right)\right] \quad , \qquad (9)$$

where δ is the drag parameter, ρ_o the density at distance r_o when $\phi_p = 90^\circ$, and $z = ae/H \simeq 115e$ here, with $H = 60$ km, so that z is generally of order 0.3. The term $F \cos \phi_p$ in equation (9) expresses the effect of the day-to-night variation in density: here the appropriate value of F is about 0.6 (see Table 7.1 of Ref 4), and the geocentric angle ϕ_p between the perigee and the centre of the 'diurnal bulge' goes through six cycles. As a first approximation, therefore, ignoring the F-term in (9) is equivalent to ignoring a six-cycle oscillation having an average amplitude twice as large as the spherical-atmosphere term (because $F \simeq 2z$). The maximum effect caused by the day-to-night variation is $2/\pi$ times twice the spherical-atmosphere effect over a half-cycle of ϕ_p, which is about one-twelfth of the total time interval. The spherical-atmosphere correction to e, which has been evaluated within THROE, is almost linear and reaches 0.000143 at the final orbit; thus it is about 0.000012 during one-twelfth of the time interval. Therefore the maximum change in e caused by the day-to-night effect is on average 0.000015 (on applying the factor $4/\pi$). This assumes that ϕ_p goes through a full cycle, but in fact the average minimum of ϕ_p in the six cycles is 45° and the average maximum 140°, so the average amplitude of the oscillation is about 25% less than estimated above, namely 0.000011. This is less than the average sd of the values, with the relaxations used in Fig 5: since $\varepsilon = 2.63$, the inclusion of the effects of the day-to-night variation would be unlikely to have a significant effect.

However, it so happens that between MJD 45766 and 45805, at the start of the ill-fitting region in Fig 5, the perigee is continually within 90° of the centre of the bulge, and the day-to-night effect is unusually large, increasing to about 0.000030. However, the points between MJD 45790 and 45814 demand a correction of 0.000150 to bring them close to the curve; so even this extra-large correction is much less than required, though it would slightly improve the fitting.

It can be concluded that the fitting in Fig 5 would not be much improved by taking account of the day-to-night variation in air density. If, in future, a better analysis can be made through improvements in the THROE program, the day-to-night correction would be worth making.

9 THE ACCURACY OF THE LUMPED HARMONICS, IN TERMS OF GEOID HEIGHT

The standard deviations σ of the values of lumped harmonics in equations (6) and (7) can be approximately interpreted as equivalent to accuracies σ_g, say, in geoid height. The linking equation is $\sigma_g \simeq R\sigma/\bar{Q}$,

where $$\bar{Q} = \left\{ \sum_{\ell} \left(Q_{\ell}^{q,k} \ell_o^2 / \ell^2 \right)^2 \right\}^{\frac{1}{2}} ,$$

on the assumption that the magnitudes of the individual coefficients fall off as $1/\ell^2$. The numerical values of the Q coefficients for 1968-70A are listed in the Appendix, and the values of σ_g for the lumped harmonics in equations (6) and (7) are as follows.

Table 3

σ_g for 15th-order lumped harmonics

Harmonic	$\bar{C}_{15}^{0,1}$	$\bar{S}_{15}^{0,1}$	$\bar{C}_{15}^{1,0}$	$\bar{S}_{15}^{1,0}$	$\bar{C}_{15}^{-1,2}$	$\bar{S}_{15}^{-1,2}$
σ_g (cm)	0.7	0.55	1.8	1.3	2.0	1.5

Table 4

σ_g for 30th-order lumped harmonics

Harmonic	$\bar{C}_{30}^{0,2}$	$\bar{S}_{30}^{0,2}$	$\bar{C}_{30}^{1,1}$	$\bar{S}_{30}^{1,1}$	$\bar{C}_{30}^{-1,3}$	$\bar{S}_{30}^{-1,3}$
σ_g (cm)	2.4	1.7	3.7	7.1	5.3	8.1

Thus it appears that the 15th-order lumped harmonics determined from the inclination have accuracies equivalent to about 0.6 cm in geoid height, while those determined from eccentricity have an average accuracy of 1.6 cm in geoid height. For the 30th-order lumped harmonics the corresponding accuracies are 2 cm and 6 cm.

10 CONCLUSIONS

The orbit of 1968-70A was significantly influenced by the effects of 15th- and 30th-order harmonics in the geopotential during all the 15 months over which the orbit was determined, from 4 July 1983 to 30 October 1984. The orbit determinations were at 77 epochs, and utilized 4744 observations including 284 Hewitt camera observations: the accuracy achieved was fairly uniform, the average

standard deviations in inclination and eccentricity being about 85 m and 65 m respectively. This is the most accurate and most extensive orbit to be analysed at 15th-order resonance at an inclination near 56°.

Analysis of the variation in orbital inclination (Fig 4) has yielded values of lumped harmonics of order 15 and 30, given in equations (6), which have standard deviations equivalent to accuracies in geoid height of 0.6 cm and 2.0 cm respectively. Analysis of the variation in orbital eccentricity gave values of two pairs of lumped harmonics of order 15 and two of order 30: see equations (7). The fitting of eccentricity was less than perfect (see Fig 5), but the accuracies were still good, being equivalent to an average of 1.6 cm in geoid height for 15th order and 6 cm for 30th order. The results have already been used[6] to improve the determination of the individual harmonic coefficients of order 15 and 30.

Appendix

VALUES OF THE Q COEFFICIENTS FOR 1968-70A

The Q coefficients $Q_\ell^{q,k}$ determine the numerical dependence of the lumped harmonic $C_m^{q,k}$ on the individual harmonic coefficients $\bar{C}_{\ell m}$, as indicated in equation (4). For $m = 15$ and $(q,k) = (0,1)$, for example,

$$\bar{C}_{15}^{0,1} = \bar{C}_{15,15} + Q_{17}^{0,1}\bar{C}_{17,15} + Q_{19}^{0,1}\bar{C}_{19,15} + \cdots\cdots .$$

For $m = 15$ and $(q,k) = (1,0)$, the first term has ℓ even, and

$$\bar{C}_{15}^{1,0} = \bar{C}_{16,15} + Q_{18}^{1,0}\bar{C}_{18,15} + Q_{20}^{1,0}\bar{C}_{20,15} + \cdots\cdots .$$

The equations are similar for $\bar{S}_{\ell m}$, substituting S for C. The values of the relevant Q coefficients are tabulated below.

Table 5

Values of $Q_\ell^{q,k}$ for 15th order (m = 15)

(q,k) = (0,1)		(q,k) = (1,0)		(q,k) = (-1,2)	
ℓ	Q	ℓ	Q	ℓ	Q
15	1.000	16	1.000	16	1.000
17	-4.337	18	-3.145	18	-1.742
19	5.056	20	3.405	20	0.280
21	-0.218	22	0.126	22	1.189
23	-2.845	24	-2.395	24	-0.007
25	-0.078	26	-0.107	26	-0.902
27	1.782	28	1.756	28	-0.334
29	0.553	30	0.502	30	0.553
31	-0.988	32	-1.169	32	0.519
33	-0.755	34	-0.806	34	-0.168
35	0.348	36	0.563	36	-0.491
37	0.673	38	0.860	38	-0.136
39	0.081	40	-0.030	40	0.305

Table 6

Values of $Q_{\ell}^{q,k}$ for 30th order (m = 30)

(q,k) = (0,2)		(q,k) = (1,1)		(q,k) = (-1,3)	
ℓ	Q	ℓ	Q	ℓ	Q
30	1.000	31	1.000	31	1.000
32	-8.756	33	-5.683	33	-4.362
34	26.447	35	14.752	35	8.045
36	-38.430	37	-19.658	37	-5.902
38	21.820	39	9.670	39	-1.795
40	10.542	41	7.296	41	4.672
42	-17.172	43	-9.471	43	0.671
44	-4.024	45	-3.231	45	-3.392
46	11.453	47	7.066	47	-0.838
48	3.345	49	2.498	49	2.364
50	-7.300	51	-4.925	51	1.188

Table 2

ORBITAL PARAMETERS FOR COSMOS 236 AT THE 77 EPOCHS, WITH STANDARD DEVIATIONS

	MJD	Date	a	e	i	Ω	ω	M_0	M_1	M_2	M_3	ε	N	D	a(1 - e)
1	45519*	1983 July 4	6886.0143 2	0.001930 4	56.0663 3	261.617 1	56.7 3	302.1 3	5469.7072 2	0.0063 2	-	0.36	44	5.3	6872.72
2	45523*	July 8	6885.9645 1	0.002029 10	56.0651 6	244.605 2	56.3 7	230.0 7	5469.7664 1	0.0087 2	-	0.88	33	2.5	6871.99
3	45527*	July 12	6885.9119 5	0.002100 6	56.0607 5	227.587 1	63.4 5	150.7 5	5469.8288 6	0.0068 6	-	0.67	46	3.8	6871.45
4	45531*	July 16	6885.8321 7	0.002233 9	56.0630 5	210.574 1	68.4 5	73.6 5	5469.9240 8	0.0112 7	-0.0015 4	0.65	64	3.8	6870.46
5	45536*	July 21	6885.7098 6	0.002331 12	56.0602 7	189.301 2	71.5 5	71.1 5	5470.0695 7	0.0152 4	-	0.90	78	5.9	6869.66
6	45541*	July 26	6885.5553 7	0.002462 13	56.0668 7	168.029 2	75.5 5	68.6 5	5470.2542 9	0.0166 2	-	0.69	40	4.9	6868.60
7	45546*	July 31	6885.4228 2	0.002509 11	56.0689 8	146.759 2	81.1 5	65.2 5	5470.4124 3	0.0152 1	-	0.67	47	4.7	6868.15
8	45552*	August 6	6885.2770 5	0.002577 11	56.0731 11	121.230 2	87.1 4	135.0 4	5470.5865 6	0.0112 3	-	0.64	54	5.6	6867.53
9	45559	August 13	6885.1047 4	0.002569 9	56.0704 13	91.450 1	95.2 4	276.6 4	5470.7916 5	0.0149 2	-	0.54	44	6.9	6867.42
10	45565	August 19	6884.9725 3	0.002532 8	56.0682 10	65.919 1	102.3 3	347.6 3	5470.9490 4	0.0126 2	-	0.48	49	6.8	6867.54
11	45573	August 27	6884.8099 4	0.002374 8	56.0648 10	31.869 1	110.5 3	204.8 3	5471.1425 4	0.0096 2	-	0.47	49	6.3	6868.47
12	45580	September 3	6884.7039 2	0.002203 9	56.0649 9	2.075 1	117.0 3	351.5 3	5471.2689 3	0.0090 1	-	0.38	46	6.3	6869.54
13	45586	September 9	6884.5949 3	0.002005 9	56.0638 8	336.537 1	122.0 3	67.3 3	5471.3987 4	0.0144 2	-	0.41	57	5.3	6870.79
14	45591	September 14	6884.4851 4	0.001853 11	56.0627 9	315.253 1	126.1 3	71.2 3	5471.5295 5	0.0127 4	-	0.43	62	4.4	6871.17
15	45597*	September 20	6884.3406 4	0.001724 14	56.0625 4	289.710 1	132.9 4	146.9 4	5471.7018 5	0.0151 3	-	0.62	51	5.4	6872.47
16	45603	September 26	6884.1987 4	0.001508 14	56.0637 9	264.162 1	134.0 5	229.2 5	5471.8711 5	0.0160 3	-	0.55	60	4.9	6873.82
17	45608*	October 1	6884.0701 4	0.001291 9	56.0668 3	242.877 1	134.2 5	239.5 5	5472.0247 5	0.0136 3	-	0.52	60	4.9	6875.18
18	45613*	October 6	6883.9159 5	0.001158 11	56.0680 3	221.585 1	138.0 7	246.8 7	5472.2087 6	0.0190 3	-	0.57	54	5.6	6875.94
19	45619	October 12	6883.7104 4	0.000971 16	56.0709 12	196.038 2	140.2 1.0	331.4 1.0	5472.4540 5	0.0220 4	-	0.63	57	5.6	6877.03
20	45625	October 18	6883.4808 8	0.000752 13	56.0718 10	170.492 1	136.7 9	63.2 9	5472.7279 9	0.0183 3	-0.0009 1	0.58	67	6.6	6878.30

Table 2 (continued)

	MJD	Date	a	e	i	Ω	ω	M_o	M_1	M_2	M_3	ε	N	D	a(1 - e)
21	45632*	1983 October 25	6883.3395 3	0.000476 4	56.0699 9	140.683 1	124.4 9	240.2 9	5472.8962 3	0.0086 2	-	0.34	48	6.5	6880.06
22	45640	November 2	6883.1871 2	0.000333 7	56.0678 10	106.610 1	96.8 1.9	148.6 1.9	5473.0778 3	0.0139 2	-	0.38	46	6.3	6880.89
23	45647*	November 9	6883.0159 4	0.000427 10	56.0662 5	76.790 1	53.7 1.9	358.8 1.9	5473.2818 5	0.0173 3	-	0.60	59	6.3	6880.08
24	45654*	November 16	6882.8432 2	0.000568 8	56.0655 3	46.972 1	42.1 8	179.2 8	5473.4878 2	0.0104 1	-	0.42	68	6.3	6878.93
25	45660*	November 22	6882.7699 9	0.000782 9	56.0645 3	21.409 1	39.8 8	275.5 8	5473.5751 11	0.0045 3	-0.0006 1	0.59	73	6.3	6877.39
26	45667	November 29	6882.7251 3	0.001059 9	56.0580 5	351.583 1	38.7 5	86.6 5	5473.6280 3	0.0068 2	-	0.41	66	6.4	6875.44
27	45674	December 6	6882.6338 4	0.001329 15	56.0542 10	321.752 1	41.5 7	254.5 7	5473.7365 5	0.0109 2	-	0.59	46	6.3	6873.49
28	45681	December 13	6882.4863 4	0.001557 11	56.0549 8	291.918 1	47.1 5	60.6 5	5473.9125 5	0.0149 2	-	0.53	61	6.9	6871.77
29	45689	December 21	6882.3402 2	0.001841 8	56.0560 7	257.823 1	53.0 4	303.8 4	5474.0870 3	0.0082 1	-	0.46	64	6.6	6869.67
30	45696	December 28	6882.2395 2	0.002079 9	56.0549 9	227.987 1	58.8 4	112.0 4	5474.2070 3	0.0092 1	-	0.58	68	7.6	6867.93
31	45703	1984 January 4	6882.1159 3	0.002315 8	56.0548 10	198.148 1	63.8 4	281.9 4	5474.3545 4	0.0112 2	-	0.60	56	7.0	6866.18
32	45710	January 11	6881.9887 5	0.002498 9	56.0565 14	168.307 1	69.8 5	91.8 5	5474.5064 6	0.0122 4	-	0.62	54	5.4	6864.80
33	45716*	January 17	6881.8692 3	0.002629 8	56.0649 3	142.732 1	75.5 3	186.4 3	5474.6498 3	0.0103 2	-	0.56	68	5.4	6863.78
34	45723	January 24	6881.7307 3	0.002740 9	56.0694 9	112.894 1	82.2 2	357.7 2	5474.8155 4	0.0122 2	-	0.65	56	6.5	6862.87
35	45728*	January 29	6881.6146 3	0.002761 5	56.0713 7	91.58[illegible] 1	87.3 1	17.6 1	5474.9542 4	0.0162 4	-	0.62	72	4.4	6862.61
36	45733*	February 3	6881.4974 10	0.002795 6	56.0719 5	70.272 1	92.7 3	38.1 3	5475.0941 13	0.0142 7	0.0031 6	0.51	62	3.4	6862.26
37	45737	February 7	6881.3879 5	0.002813 8	56.0740 12	53.218 1	96.4 4	343.5 4	5475.2251 6	0.0142 4	-	0.46	33	4.4	6862.03
38	45742*	February 12	6881.2508 2	0.002779 5	56.0740 6	31.904 1	101.8 2	5.2 2	5475.3887 3	0.0203 3	-	0.42	69	4.9	6862.13
39	45747*	February 17	6881.0944 4	0.002724 7	56.0775 3	10.589 1	107.3 3	27.9 3	5475.5757 4	0.0160 6	-	0.48	50	3.9	6862.35
40	45751*	February 21	6880.9752 4	0.002672 6	56.0822 8	353.534 1	111.2 2	335.0 2	5475.7184 5	0.0203 4	-	0.40	47	4.1	6862.59

Table 2 (continued)

	MJD	Date	a	e	i	Ω	ω	M_0	M_1	M_2	M_3	ε	N	D	a(1 - e)
41	45758	1984 February 28	6880.7169 2	0.002556 6	56.0839 9	323.696 1	119.2 2	152.9 2	5476.0269 2	0.0245 1	-	0.41	67	7.6	6863.13
42	45766	March 7	6880.3950 2	0.002344 8	56.0837 9	289.590 1	126.8 3	52.2 3	5476.4112 3	0.0200 1	-	0.52	89	7.9	6864.27
43	45774	March 15	6880.1388 5	0.002036 10	56.0833 9	255.478 1	133.7 3	314.9 3	5476.7170 6	0.0210 1	0.0005 1	0.51	59	8.0	6866.13
44	45782	March 23	6879.7867 3	0.001728 11	56.0869 9	221.360 1	142.6 4	218.4 4	5477.1378 3	0.0296 1	-	0.53	65	7.4	6867.90
45	45790*	March 31	6879.3715 5	0.001326 10	56.0926 3	187.246 1	148.8 4	128.2 4	5477.6343 6	0.0315 1	-0.0006 1	0.59	82	7.4	6870.25
46	45798	April 8	6878.9929 5	0.001020 11	56.0932 8	153.125 1	157.2 4	39.7 4	5478.0865 6	0.0225 1	-0.0006 1	0.46	72	7.4	6871.98
47	45805*	April 15	6878.7881 6	0.000706 11	56.0957 3	123.264 1	161.5 6	237.8 6	5478.3315 7	0.0157 2	-0.0005 1	0.47	80	5.7	6873.93
48	45810*	April 20	6878.6393 4	0.000363 17	56.0961 3	101.926 1	164.5 1.2	277.5 1.1	5478.5092 4	0.0202 7	-	0.73	75	3.9	6876.14
49	45814*	April 24	6878.5074 3	0.000259 25	56.0974 8	84.868 3	154.6 3.9	250.2 3.9	5478.6670 4	0.0219 2	-	0.79	58	3.9	6876.73
50	45818*	April 28	6878.3241 3	0.000168 18	56.1012 4	67.810 2	163.8 3.5	204.7 3.5	5478.8863 4	0.0221 3	-0.0035 3	0.72	70	3.9	6877.17
51	45823*	May 3	6878.1553 4	0.000222 15	56.1078 6	46.478 2	48.8 4.5	5.2 4.5	5479.0886 2	0.0183 2	-0.0017 1	0.62	58	5.6	6876.63
52	45830	May 10	6878.0003 4	0.000603 9	56.1101 6	16.618 1	31.6 7	231.5 7	5479.2741 5	0.0134 1	0.0004 <1	0.37	62	7.6	6873.85
53	45838	May 18	6877.8031 4	0.001040 10	56.1088 8	342.488 1	30.5 5	164.7 5	5479.5096 5	0.0162 1	0.0003 1	0.43	53	7.9	6870.65
54	45846	May 26	6877.5684 3	0.001391 8	56.1083 5	308.355 1	36.3 3	93.1 3	5479.7901 4	0.0150 1	-0.0002 <1	0.34	51	7.4	6868.00
55	45854	June 3	6877.4035 1	0.001720 8	56.1106 5	274.218 1	42.1 3	23.5 3	5479.9873 2	0.0098 1	-	0.28	44	7.3	6865.57
56	45861	June 10	6877.3160 2	0.001941 7	56.1094 5	244.348 1	48.2 2	232.5 2	5480.0919 2	0.0047 1	-	0.26	42	5.3	6863.97
57	45867*	June 16	6877.2696 6	0.002104 8	56.1029 4	218.742 1	53.7 3	0.5 3	5480.1467 7	0.0053 2	-0.0006 1	0.45	54	5.8	6862.80
58	45872*	June 21	6877.2298 4	0.002234 10	56.1034 6	197.401 1	59.2 3	46.4 3	5480.1943 5	0.0047 6	-	0.65	61	3.8	6861.87
59	45877*	June 26	6877.1890 2	0.002253 16	56.0953 6	176.054 2	66.4 6	91.0 6	5480.2424 3	0.0048 3	-	0.70	42	4.9	6861.69
60	45881*	June 30	6877.1536 6	0.002388 7	56.0939 3	158.982 1	67.4 2	59.6 2	5480.2846 8	0.0076 3	0.0009 4	0.55	69	3.9	6860.73

Table 2 (concluded)

	MJD	Date	a	e	i	Ω	ω	M_o	M_1	M_2	M_3	ε	N	D	a(1 - e)
61	45884*	1984 July 3	6877.1247 3	0.002396 14	56.0948 7	146.173 2	71.1 3	303.2 3	5480.3191 3	0.0067 2	-	0.71	42	3.0	6860.65
62	45888*	July 7	6877.0741 2	0.002435 11	56.0959 8	129.096 1	76.3 3	267.8 2	5480.3797 3	0.0108 4	-0.0008 2	0.54	50	4.6	6860.33
63	45894	July 13	6876.9968 5	0.002507 5	56.0959 6	103.476 1	82.8 3	36.6 3	5480.4722 6	0.0103 2	0.0005 1	0.47	81	5.6	6859.76
64	45901	July 20	6876.8894 2	0.002528 5	56.0970 7	73.589 1	88.8 3	249.4 3	5480.6007 2	0.0070 1	-	0.43	64	7.9	6859.50
65	45909	July 28	6876.7929 2	0.002493 6	56.0978 9	39.429 1	96.8 3	183.7 3	5480.7160 3	0.0081 1	-	0.43	50	7.9	6859.65
66	45917	August 5	6876.6641 2	0.002450 5	56.1011 7	5.268 1	104.9 3	118.8 3	5480.8703 2	0.0101 1	-	0.43	70	7.4	6859.82
67	45925	August 13	6876.5256 2	0.002378 10	56.1071 8	331.112 1	112.7 3	55.6 3	5481.0365 3	0.0104 1	-	0.51	78	7.4	6860.17
68	45932	August 20	6876.4250 3	0.002206 12	56.1075 9	301.225 1	117.8 4	273.1 4	5481.1569 4	0.0061 3	-	0.60	88	5.4	6861.26
69	45939	August 27	6876.3636 1	0.002022 9	56.1054 5	271.338 1	123.2 3	131.0 3	5481.2301 1	0.0055 1	-	0.43	91	7.4	6862.46
70	45946	September 3	6876.3066 7	0.001794 9	56.1048 5	241.447 1	129.1 4	348.8 4	5481.2981 9	0.0051 3	0.0004 2	0.41	68	5.3	6863.97
71	45952	September 9	6876.2465 1	0.001598 7	56.1024 4	215.826 1	135.1 3	123.6 3	5481.3698 1	0.0032 1	-	0.38	73	7.0	6865.26
72	45960	September 17	6876.2223 2	0.001288 10	56.1006 7	181.663 1	142.8 4	64.0 4	5481.3986 2	0.0006 1	-	0.51	76	6.6	6867.36
73	45967	September 24	6876.1941 2	0.001017 12	56.0980 9	151.771 1	148.8 5	282.8 5	5481.4321 2	0.0052 1	-	0.48	66	7.0	6869.20
74	45978	October 5	6876.1109 1	0.000513 9	56.0923 5	104.783 1	151.0 7	120.3 7	5481.5310 2	0.0059 1	-	0.49	94	7.7	6872.58
75	45987	October 14	6875.9954 1	0.000169 4	56.0965 6	66.335 1	101.3 3.7	203.6 3.7	5481.6696 1	0.0082 1	-	0.45	99	8.9	6874.83
7[illegible]	45997	October 24	6875.8194 2	0.000481 7	56.1061 6	23.621 1	34.5 8	29.3 8	5481.8809 2	0.0106 1	-	0.46	85	7.6	6872.51
77	46003	October 30	6875.7291 3	0.000759 7	56.1067 7	357.995 1	33.5 6	174.7 6	5481.9889 4	0.0070 2	-	0.47	88	4.4	6870.51

Key:
- * = orbits containing Hewitt camera observations
- MJD = modified Julian day
- a = semi major axis (km)
- e = eccentricity
- i = inclination (degrees)
- Ω = right ascension of ascending node (degrees)
- ω = argument of perigee (degrees)
- M_o = mean anomaly at epoch (degrees)
- M_1 = mean motion n (degree/day)
- M_2, M_3 = later coefficients in the polynomial for M
- ε = measure of fit
- N = number of observations accepted
- D = time covered by the observations (days)

REFERENCES

No.	Author	Title, etc
1	D.G. King-Hele D.M.C. Walker J.A. Pilkington A.N. Winterbottom H. Hiller G.E. Perry	*The RAE table of Earth satellites 1957-1986.* Macmillan, London (1987)
2	R.H. Gooding	The evolution of the PROP6 orbit determination program, and related topics. RAE Technical Report 74164 (1974)
3	D.W. Scott	ORES: a computer program for the analysis of residuals from PROP. RAE Technical Report 69163 (1969)
4	D.G. King-Hele	*Satellite orbits in an atmosphere: theory and applications.* Chapter 6. Blackie, Glasgow (1987)
5	R.H. Gooding D.G. King-Hele	Explicit forms of some functions arising in the analysis of resonant satellite orbits. RAE Technical Report 88035 (1988)
6	D.G. King-Hele D.M.C. Walker	Evaluation of 15th- and 30th-order geopotential harmonic coefficients from 26 resonant satellite orbits. RAE Technical Report 88045 (1988)
7	G.E. Cook	PROD, a computer program for predicting the development of drag-free satellite orbits. Part 1: Theory. RAE Technical Report 71007 (1971) *Celestial Mechanics*, 7, 301-314 (1973)
8	R.H. Gooding	Lumped geopotential coefficients $\bar{C}_{15,15}$ and $\bar{S}_{15,15}$ obtained from resonant variation in the orbit of Ariel 3. RAE Technical Report 71068 (1971)
9	D.G. King-Hele D.M.C. Walker	Upper-atmosphere zonal winds from satellite orbit analysis: an update. *Planet. Space Sci.*, 36, 1085-1093 (1988) RAE Technical Report 87058 (1987)

REFERENCES (concluded)

No.	Author	Title, etc
10	D.M.C. Walker	Analyses of the US Navy orbits of 1963-24B and 1974-34A at 15th-order resonance. *Geophys. J.R. Astr. Soc.*, 67, 1-18 (1981) RAE Technical Report 80093 (1980)
11	D.M.C. Walker	Cosmos 462 (1971-106A): orbit determination and analysis. *Phil. Trans. Roy. Soc. A.*, 292, 473-512 (1979) RAE Technical Report 78089 (1978)

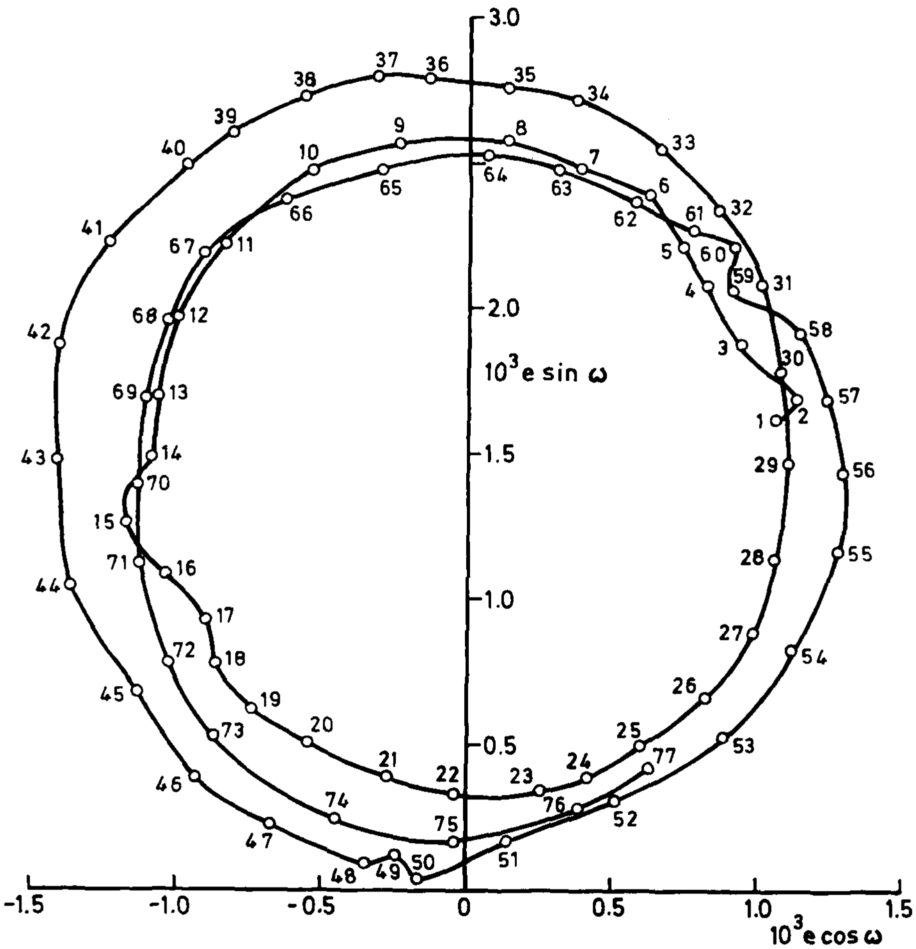

Fig 1 Values of e and ω from the 77 orbits: polar diagram

Fig 2

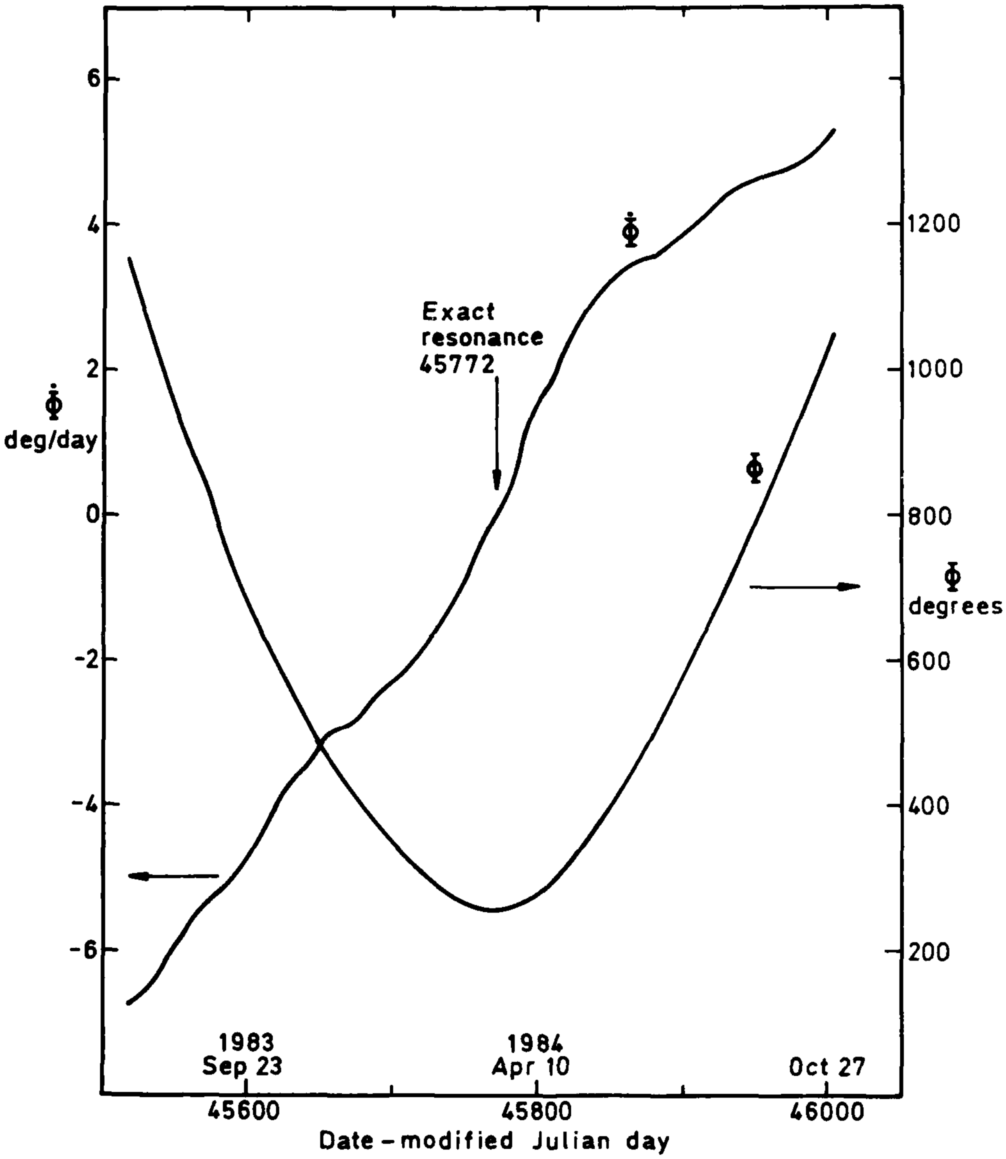

Fig 2 Variation of $\dot{\Phi}$ and Φ

TR 88058

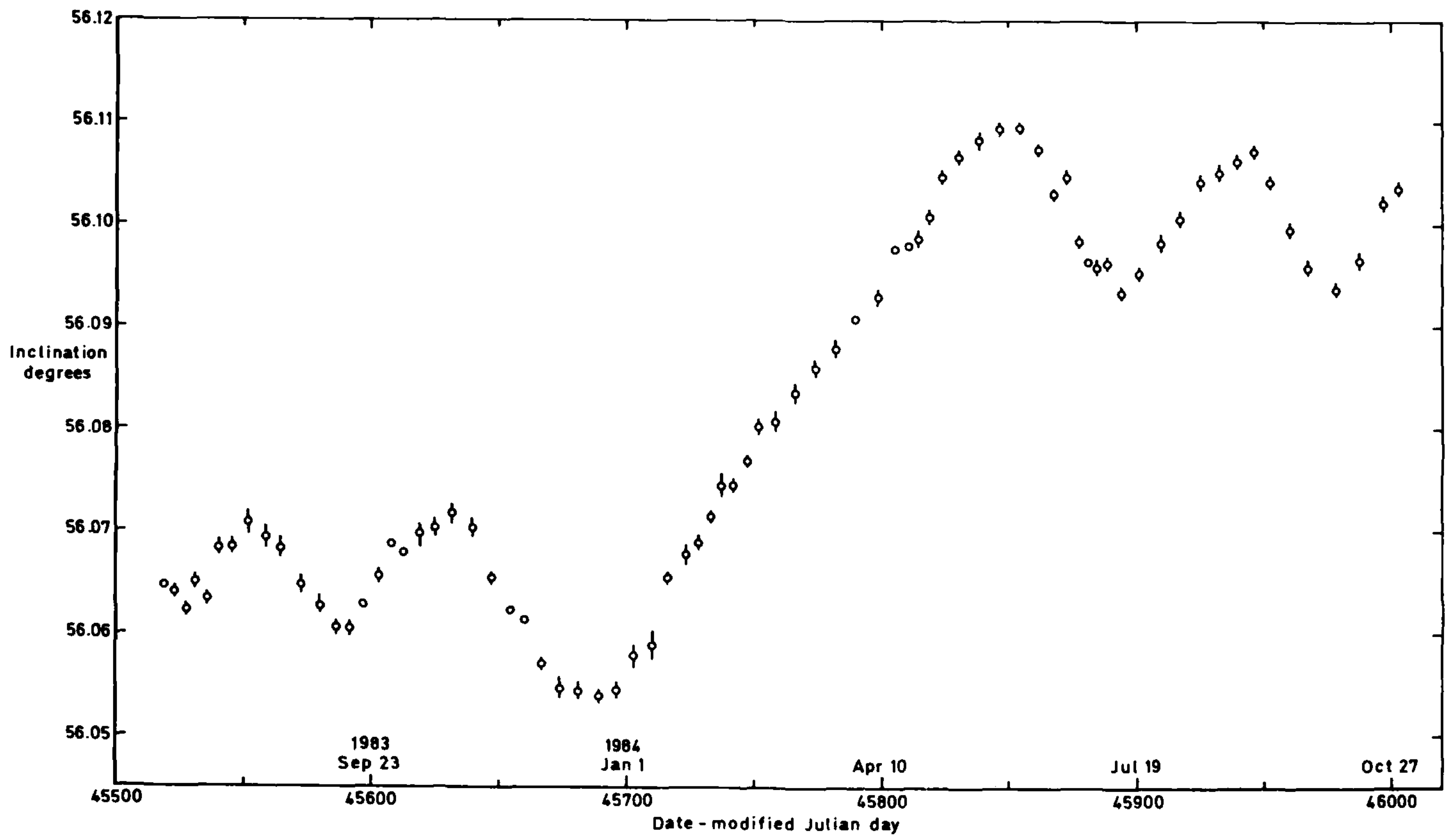

Fig 3 Values of inclination after removal of lunisolar, zonal harmonic and $J_{2,2}$ perturbations

Fig 4

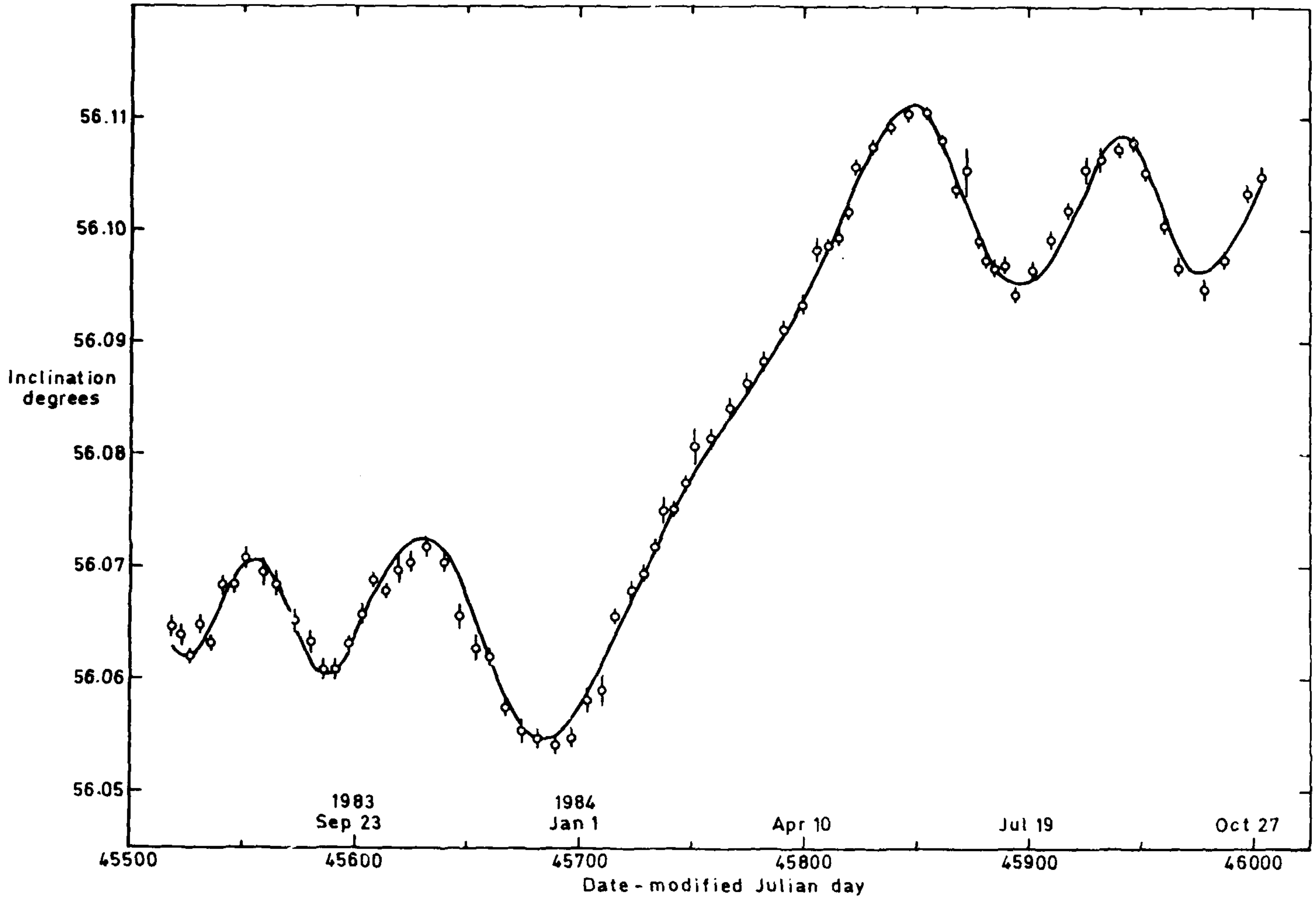

Fig 4 Values of inclination with fitted curve for $(\gamma,q) = (1,0), (2,0)$

TR 89068

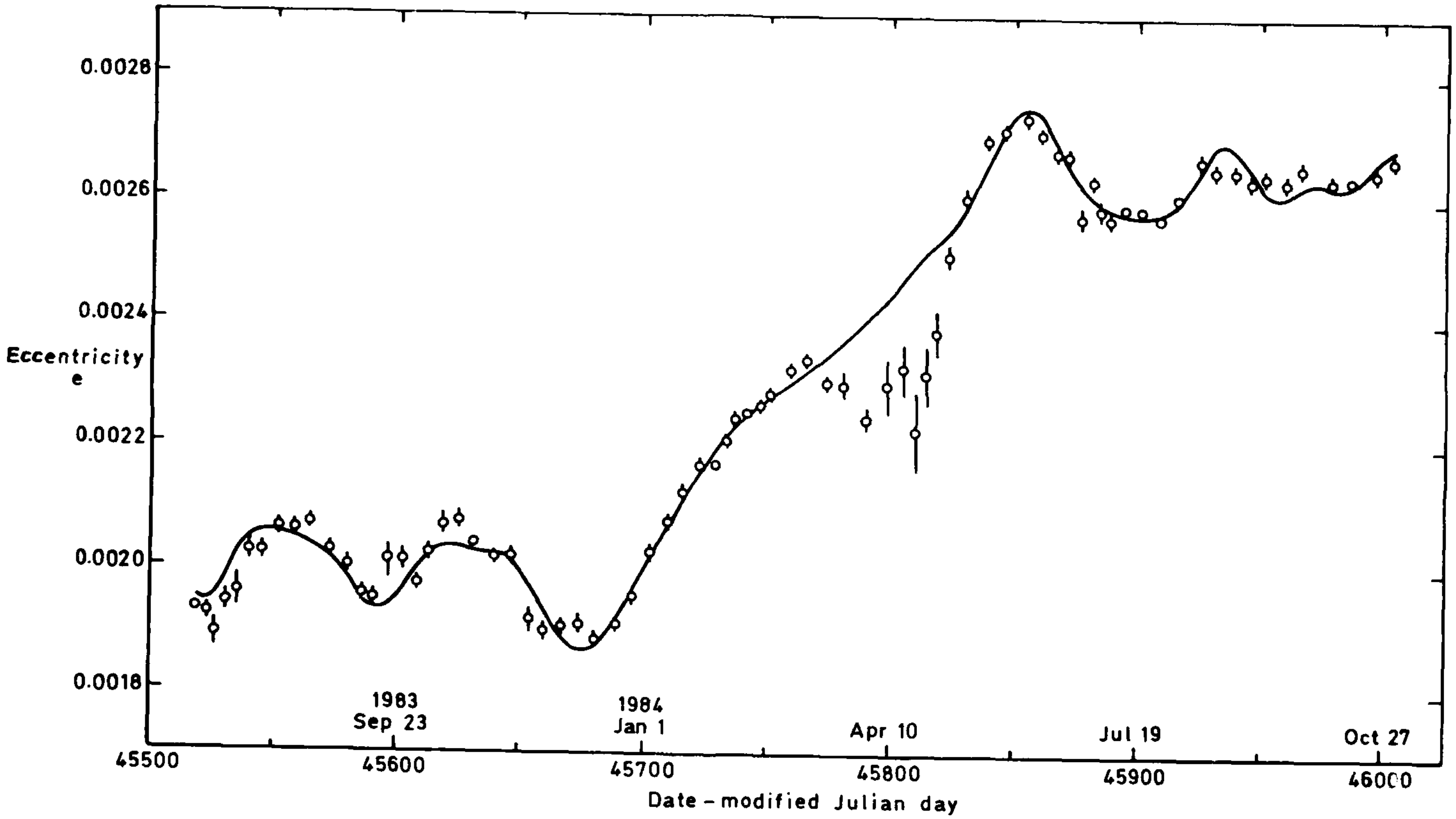

Fig 5 Values of eccentricity, after removal of perturbations, with fitting by THROE

Overall security classification of this page

UNLIMITED

As far as possible this page should contain only unclassified information. If it is necessary to enter classified information, the box above must be marked to indicate the classification, e.g. Restricted, Confidential or Secret.

1. DRIC Reference (to be added by DRIC)	2. Originator's Reference RAE TR 88058	3. Agency Reference	4. Report Security Classification/Marking UNLIMITED

5. DRIC Code for Originator 7673000W	6. Originator (Corporate Author) Name and Location Royal Aerospace Establishment, Farnborough, Hants, UK
5a. Sponsoring Agency's Code	6a. Sponsoring Agency (Contract Authority) Name and Location

7. Title
Orbit determination and analysis for Cosmos 236 at 15th-order resonance

7a. (For Translations) Title in Foreign Language

7b. (For Conference Papers) Title, Place and Date of Conference

8. Author 1. Surname, Initials Winterbottom, A.N.	9a. Author 2	9b. Authors 3, 4	10. Date September 1988	Pages 26	Refs. 11
11. Contract Number	12. Period	13. Project	14. Other Reference Nos. Special Systems 9		

15. Distribution statement
(a) Controlled by –

(b) Special limitations (if any) –

If it is intended that a copy of this document shall be released overseas refer to RAE Leaflet No.3 to Supplement 6 of MOD Manual 4.

16. Descriptors (Keywords) (Descriptors marked * are selected from TEST)
Orbital determination; Orbit analysis; Geopotential harmonics; Satellite orbits; Resonance. (edc)

17. Abstract

Cosmos 236 (1968-70A) was launched on 27 August 1968 into a near-circular orbit of inclination 56° and is expected to decay during late 1989. The orbit has been determined from observations for 77 epochs between July 1983 and October 1984 over the time interval when the orbit was expected to be significantly influenced by the effects of 15th-order resonance with the Earth's gravitational field: exact resonance occurred on 13 March 1984. The observations numbered over 4700, including 284 from the Hewitt cameras of the University of Aston which are sited at Herstmonceux in England and at Siding Spring in Australia. The orbital accuracy achieved was fairly consistent throughout, with the standard deviation in orbital inclination and eccentricity corresponding on average to positional accuracies of 85 m and 65 m respectively.

Analysis of the changes in inclination and in eccentricity at resonance has given values of three pairs of lumped harmonics of order 15 and three pairs of order 30, one pair of each from inclination and two from eccentricity. The values from inclination had standard deviations equivalent to accuracies in geoid height of 0.6 cm and 2.0 cm for orders 15 and 30 respectively while the equivalent accuracies for the values from eccentricity were 1.6 cm and 6.0 cm.